



Isotope production cross section measurements at the HFNG, LANL-IPF, and LBNL

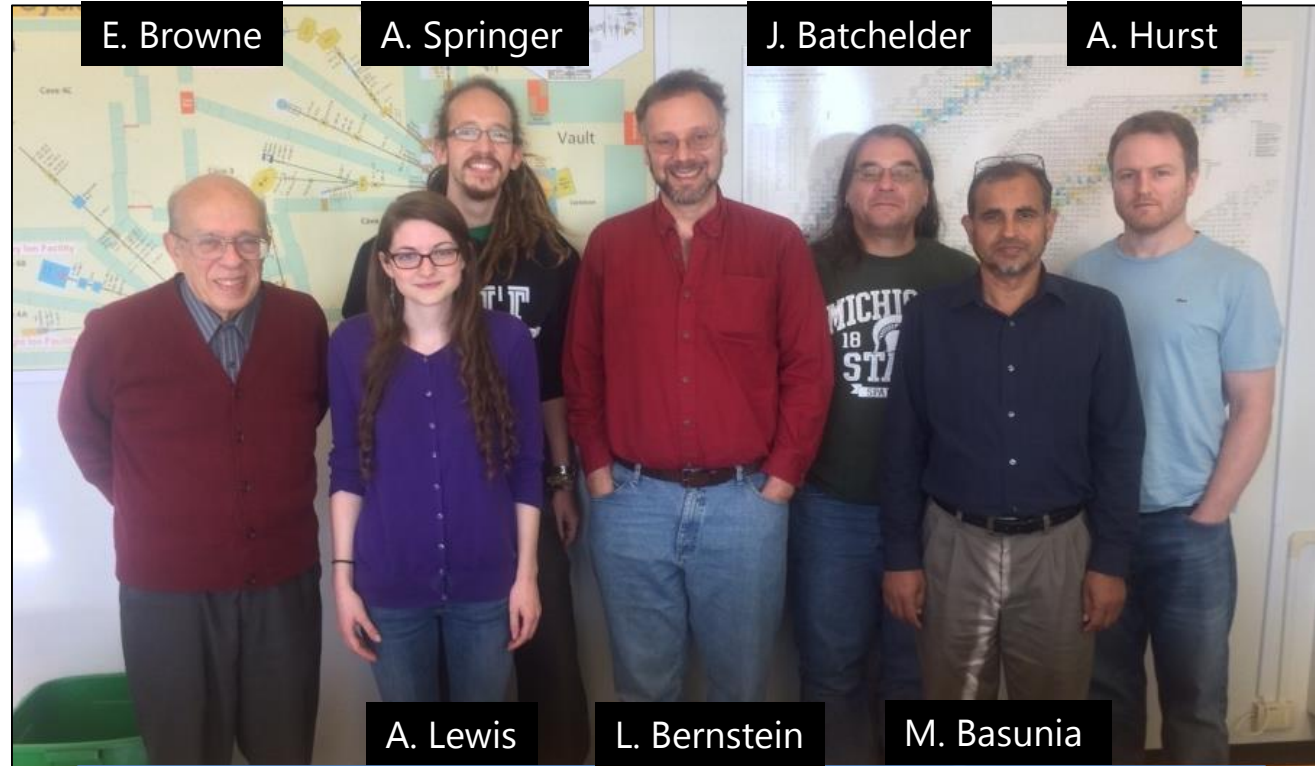
Andrew S. Voyles

24 May 2018 – 14th Nordic Meeting on Nuclear Physics

The LBNL/UCB Bay Area Nuclear Data (BAND) Group



A. Voyles



E. Browne

A. Springer

J. Batchelder

A. Hurst

A. Lewis

L. Bernstein

M. Basunia



J. Morrell

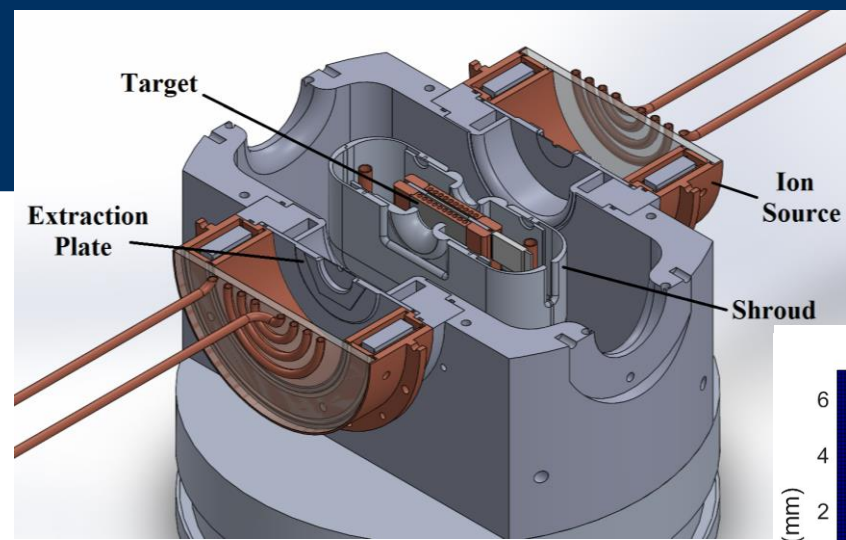
E. Matthews



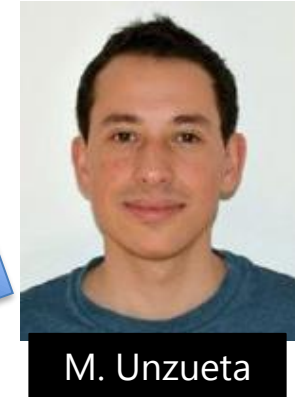
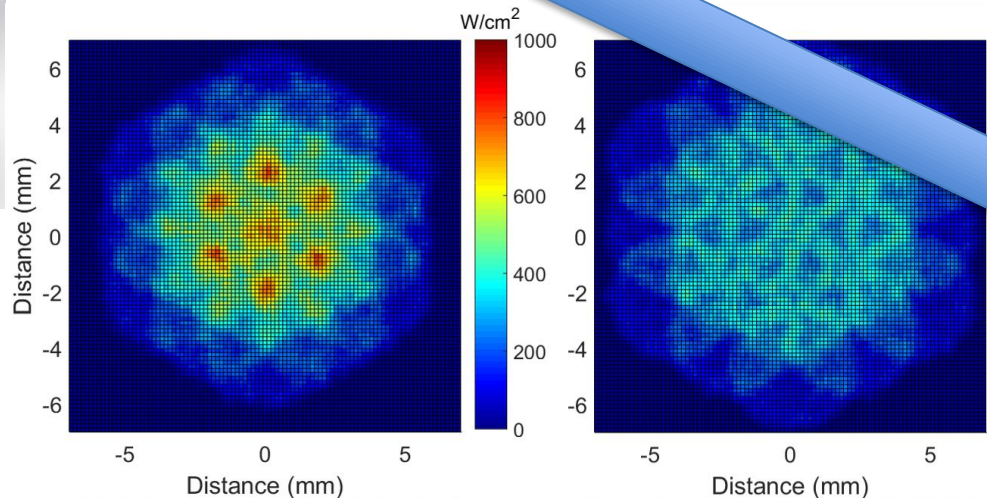
Our goal is to address the data needs of the applied nuclear science community while training the next generation of nuclear scientists and engineers in the process

Cross-Section Measurements at the UC Berkeley HFNG

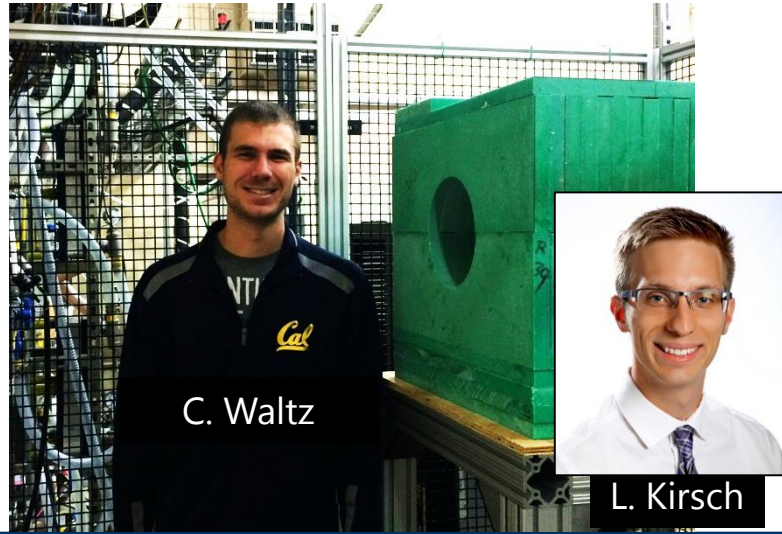
M. Allyon, "Design, construction, and characterization of a compact DD neutron generator designed for $^{40}\text{Ar}/^{39}\text{Ar}$ geochronology", NIM A (Accepted, In Press, 2018)



3 generations of our "real neutron source"

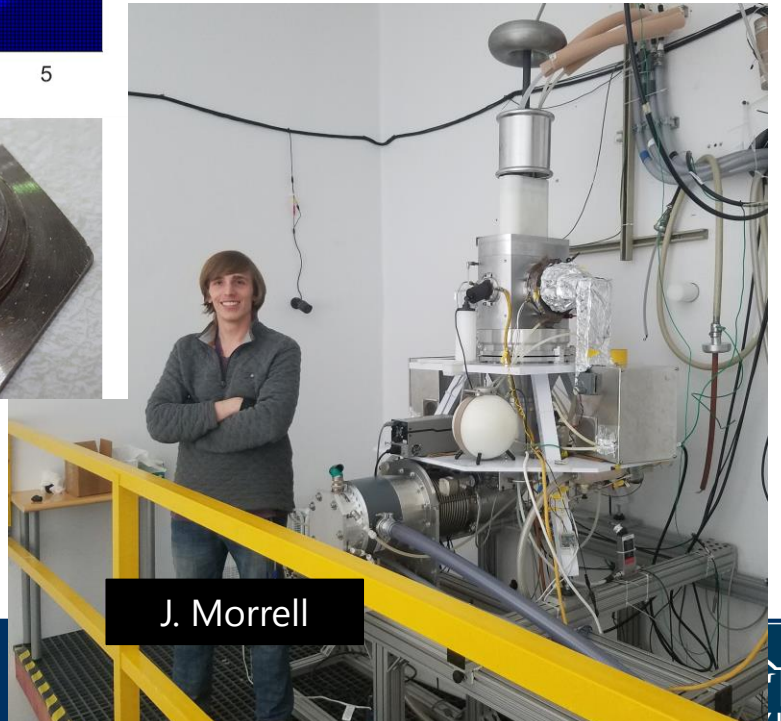
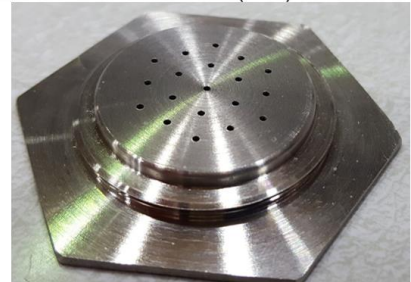
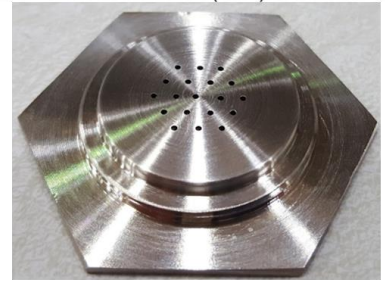


M. Unzueta



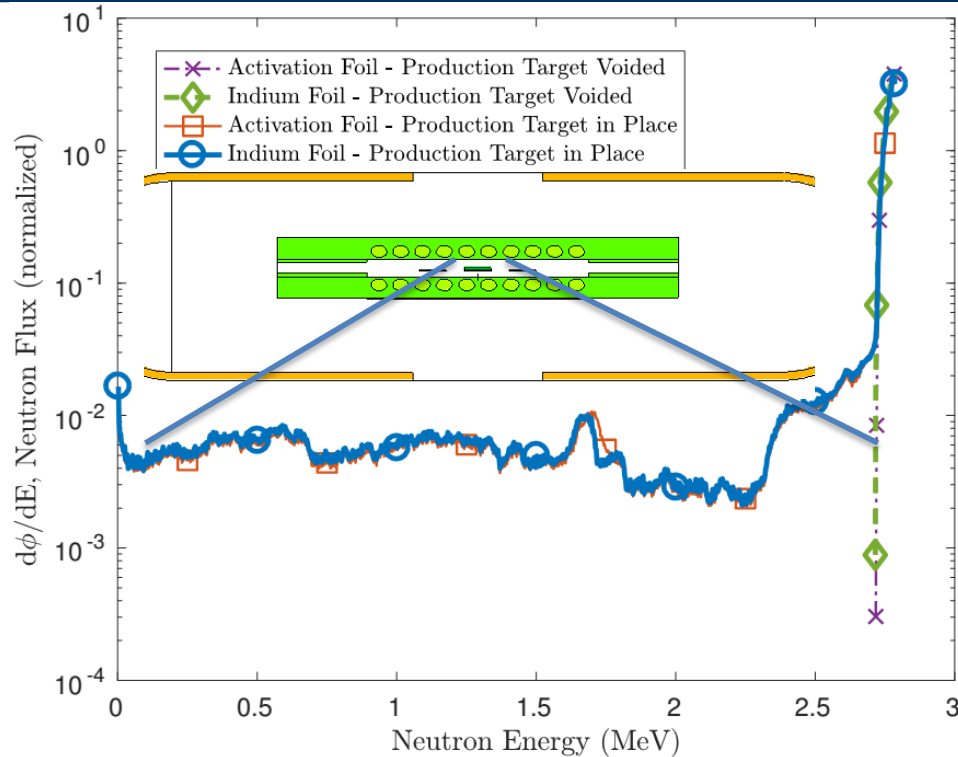
C. Waltz

L. Kirsch



J. Morrell

HFNG-Based Cross Section Measurements



Neutron flux profile modeled in target and monitor foil, using MCNP6

NDNCA Whitepaper available at <http://bang.berkeley.edu/events/ndnca/whitepaper>

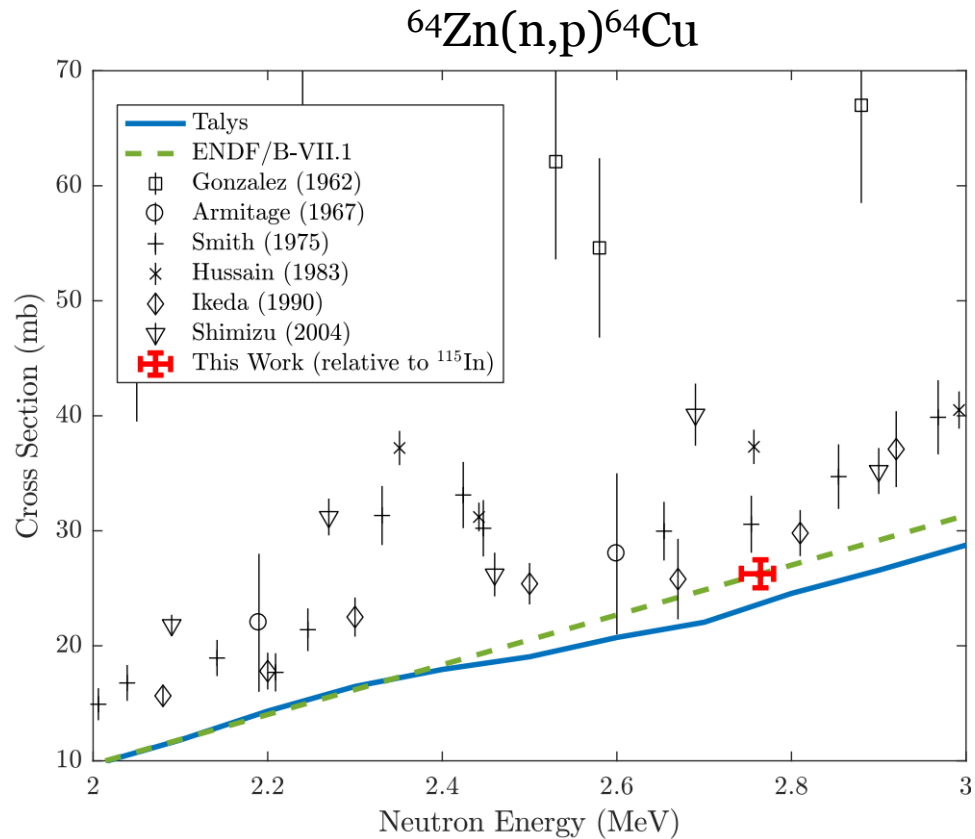
- S. Qaim called for measurements of (n,p) cross sections for the novel medical radionuclide production at NDNCA

$^{32}\text{S}(n,p)^{32}\text{P}$; $^{47}\text{Ti}(n,p)^{47}\text{Sc}$, $^{64}\text{Zn}(n,p)^{64}\text{Cu}$; $^{67}\text{Zn}(n,p)^{67}\text{Cu}$; $^{89}\text{Y}(n,p)^{89}\text{Sr}$;
 $^{105}\text{Pd}(n,p)^{105}\text{Rh}$; $^{149}\text{Sm}(n,p)^{149}\text{Pm}$, $^{153}\text{Eu}(n,p)^{153}\text{Sm}$, $^{159}\text{Tb}(n,p)^{159}\text{Gd}$; $^{161}\text{Dy}(n,p)^{161}\text{Tb}$;
 $^{166}\text{Er}(n,p)^{166}\text{Ho}$; $^{169}\text{Tm}(n,p)^{169}\text{Er}$; $^{175}\text{Lu}(n,p)^{175}\text{Yb}$; $^{177}\text{Hf}(n,p)^{177}\text{Lu}$, and several others

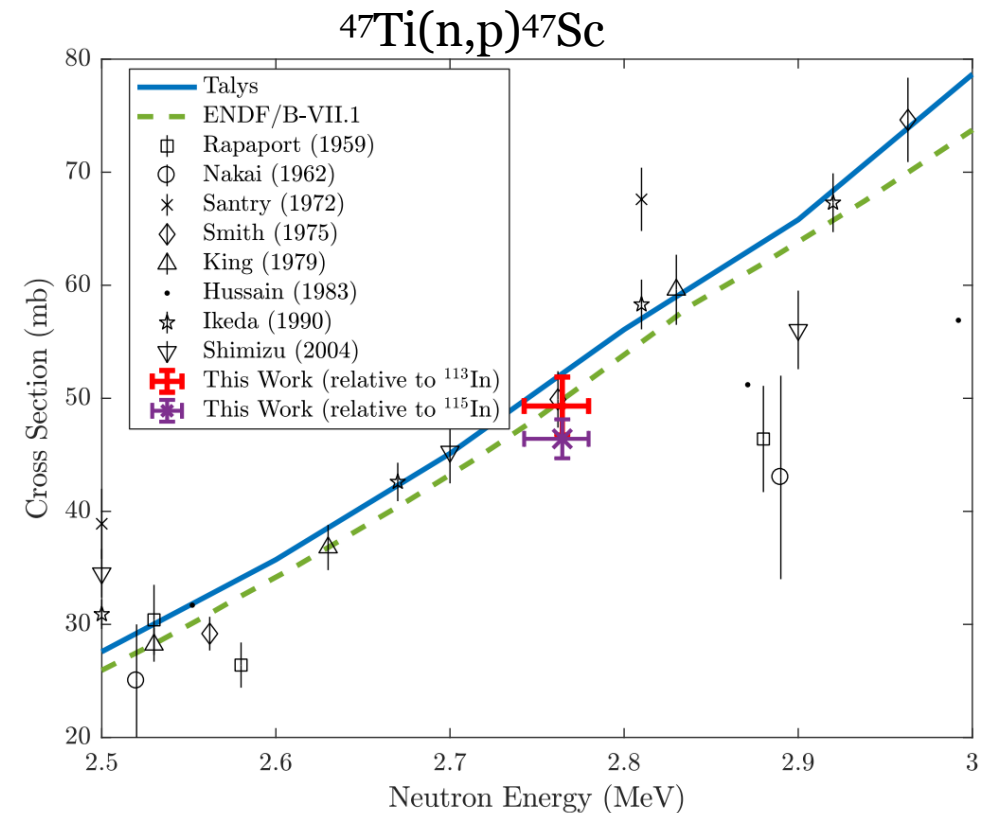
- Our paper introduces a *neutron utilization parameter* (η_n) which characterizes the effectiveness of a neutron generator as an isotope generator

Medical Applications – (n,p) ^{64}Cu , ^{47}Sc Production

- Emerging medical radionuclides
 - ^{64}Cu ($t_{1/2} = 12.7$ hr) – 61% β^+ to ^{64}Ni , 39% β^- to ^{64}Zn
 - ^{47}Sc ($t_{1/2} = 3.35$ d) – β^- to ^{47}Ti , with 159-keV γ
 - High-specific activity production

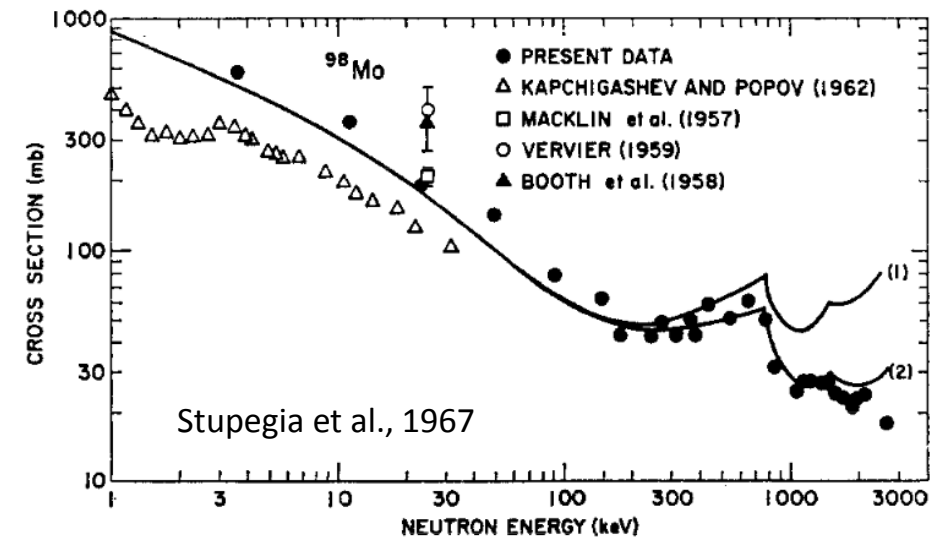


A.S. Voyles, "Measurement of the ^{64}Zn , $^{47}\text{Ti}(n,p)$ cross sections using a DD neutron generator for medical isotope studies", NIM B 410 (2017) 230–239

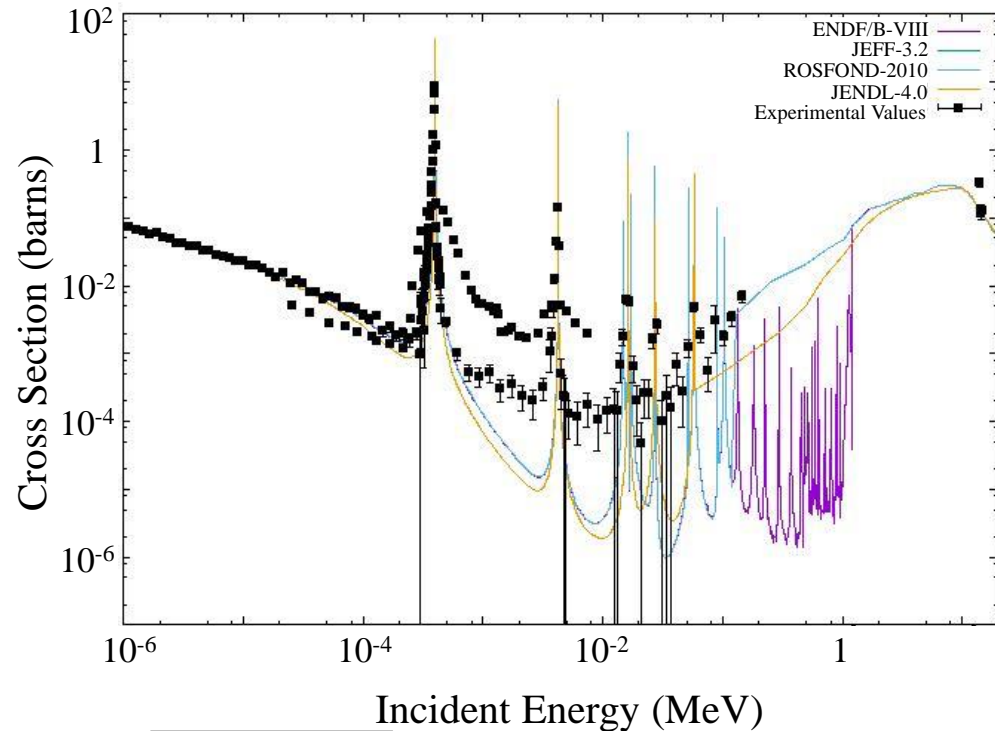


Measurement of the $^{98}\text{Mo}(n,\gamma)$ Cross Section

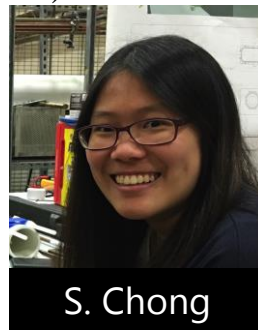
- A recent experiment at the HFNG was conducted to re-measure the (n,γ) cross section of ^{98}Mo – first measurement since 1967!
- Using a custom target holder, four energy locations were measured.
- Re-measurement of this cross section in the 1-10 MeV was marked as a vital nuclear data need in the NDNCA nuclear data needs matrix, for thermal reactor ^{99}Mo production.



Addressing large discrepancies between data libraries for $^{35}\text{Cl}(n,p)$ cross section



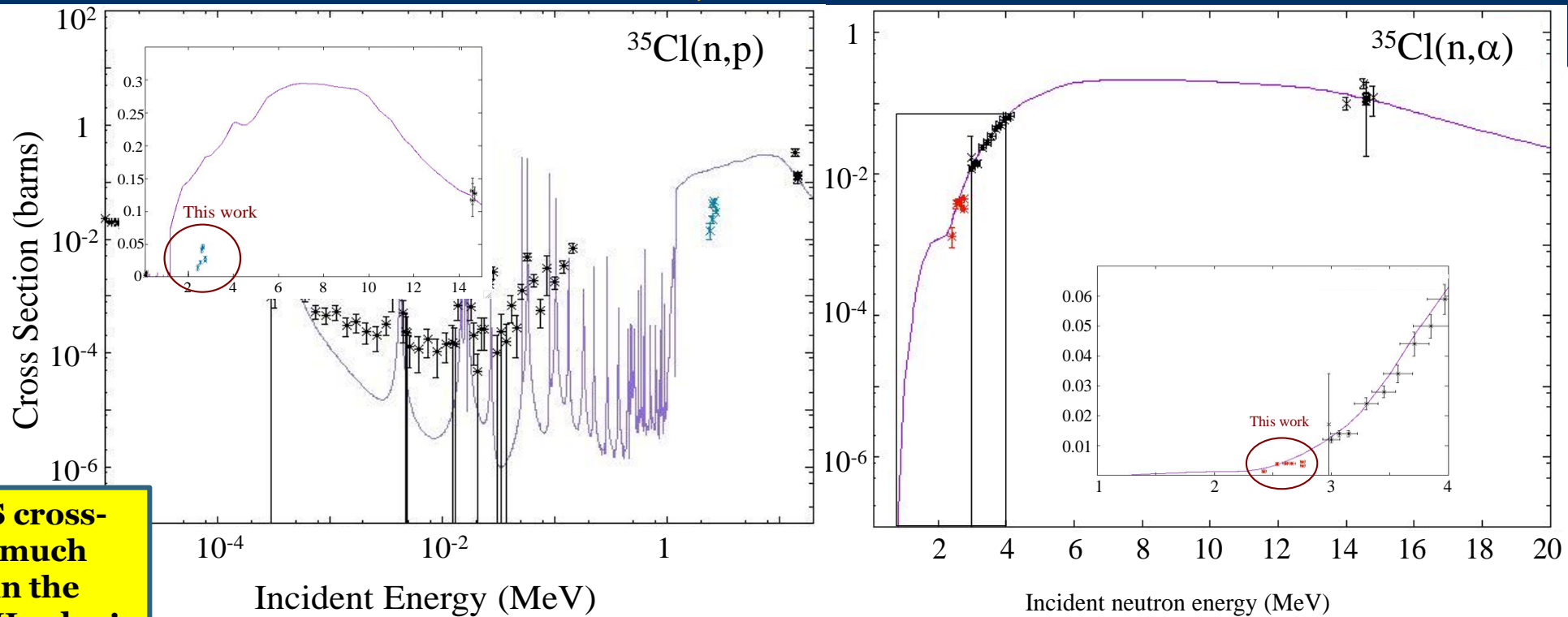
J. Batchelder



S. Chong

- ENDF/B-VII.1 (and VIII) includes detailed **calculated** resonances between 0.1 MeV and 1.2 MeV. The cross section in this region is **2-3 orders of magnitude smaller** when using ENDF/B-VII.1 vs. ENDF/B-VII.0
- Higher than 1.2 MeV, in all libraries, the cross-section is assumed to be in an Unresolved Resonance Region (URR)
- In fast neutron systems most neutrons have energies > 100 keV. There are **NO measurements between 100 keV and 14 MeV**.
- In order to decrease the uncertainties in the ^{35}Cl neutron capture, experiments were performed to measure the $^{35}\text{Cl}(n,p)^{35}\text{S}$ and the $^{35}\text{Cl}(n,\alpha)^{32}\text{P}$ cross sections using the High Flux Neutron Generator (HFNG) on the University of California Berkeley campus.

$^{35}\text{Cl}(n,x)$ Results



$^{35}\text{Cl}(n,p)^{35}\text{S}$ cross-section is much lower than the ENDF/B-VIII value!

E_n (MeV)
2.755(21)
2.661(35)
2.608(22)
2.539(6)
2.425(17)

E_n (MeV)	$\sigma(\text{mb}) \ ^{35}\text{Cl}(n,p) \ ^{35}\text{S}$	
	this work	ENDF-VIII
2.755(21)	29.5(10)	183
2.661(35)	45.7(35)	173
2.608(22)	41.1(41)	172
2.539(6)	22.3(31)	171
2.425(17)	14.1(44)	156

Poor Agreement

E_n (MeV)	$\sigma(\text{mb}) \ ^{35}\text{Cl}(n,\alpha) \ ^{32}\text{P}$	
	this work	ENDF-VIII
4.54(15)	4.54(15)	7.2
3.94(31)	3.94(31)	6.0
4.00(40)	4.00(40)	4.7
3.79(52)	3.79(52)	3.7
1.32(41)	1.32(41)	1.4

Good Agreement

Structure is observed in the $^{35}\text{Cl}(n,p)$ and $^{31}\text{P}(n,p)$ reactions. **Cannot treat the region as an unresolved resonance region!**

Stacked-target Charged Particle Excitation Functions

Low Energy – LBNL

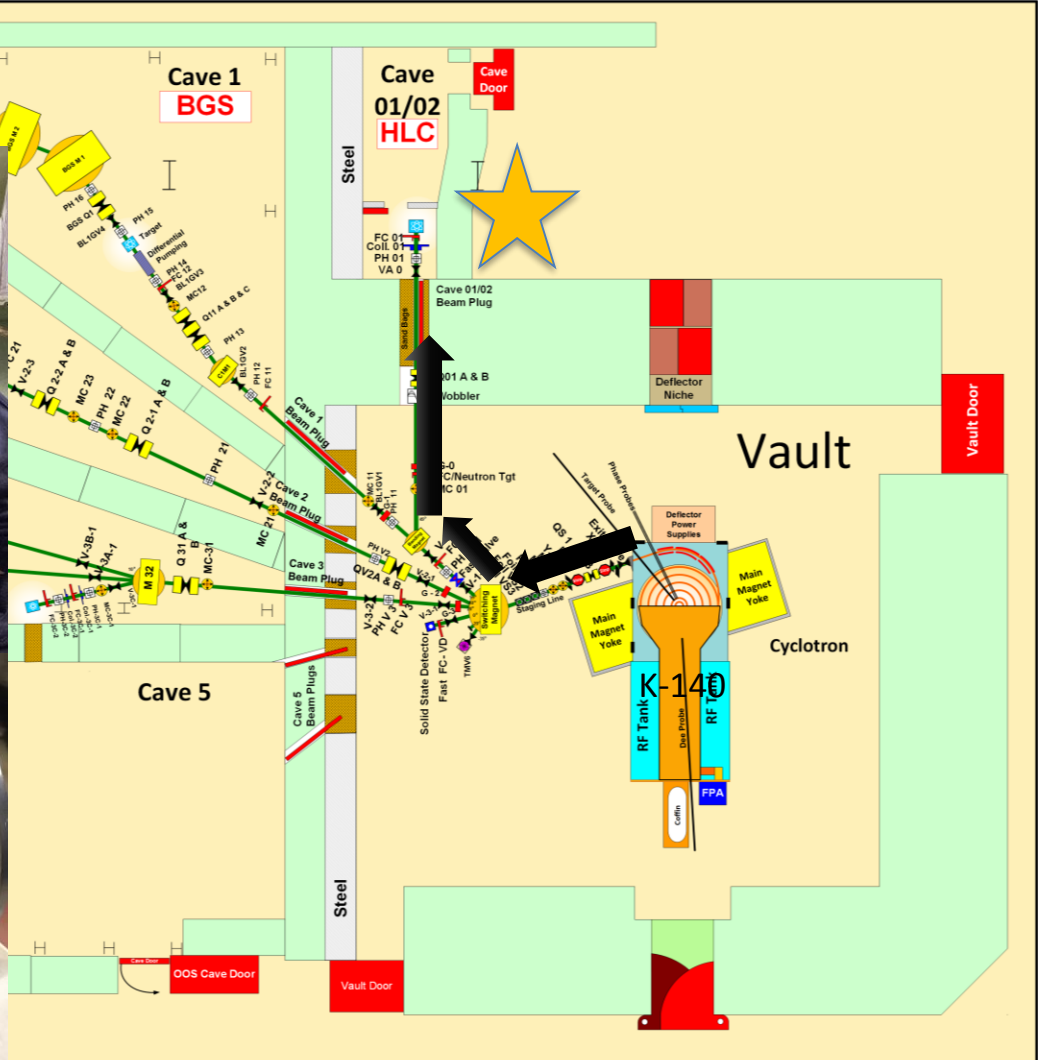
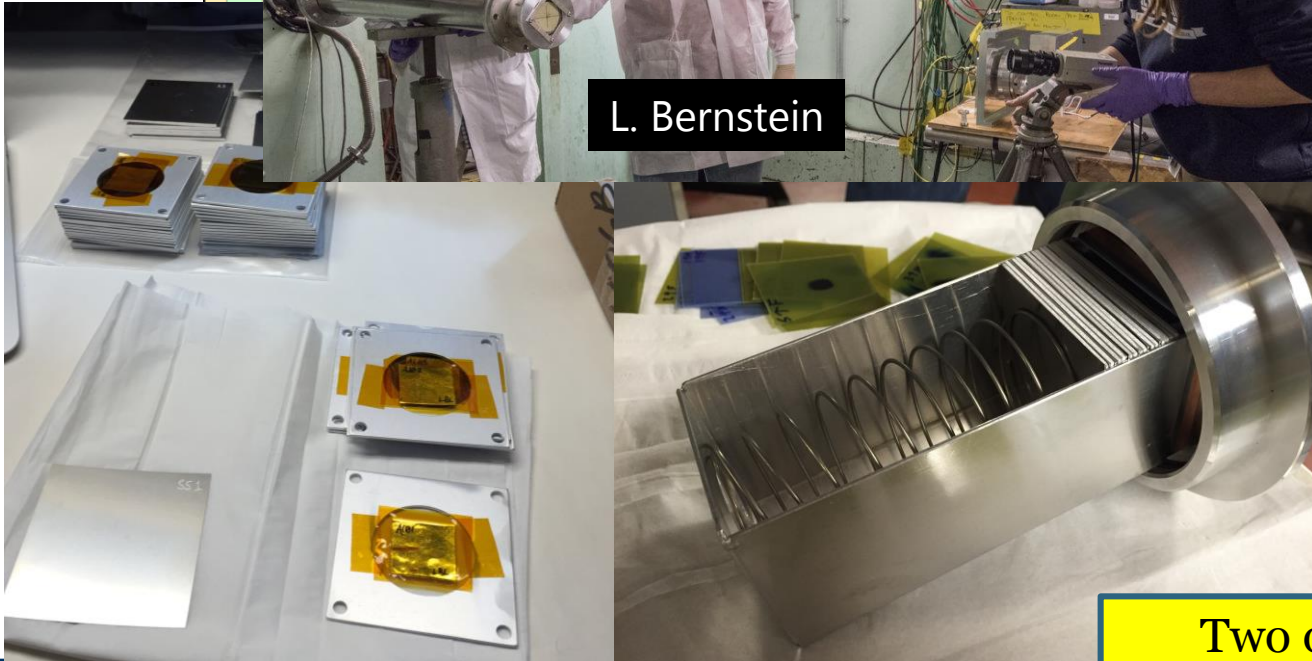
Stacked-target Charged Particle Excitation Functions

88-Inch Cyclotron



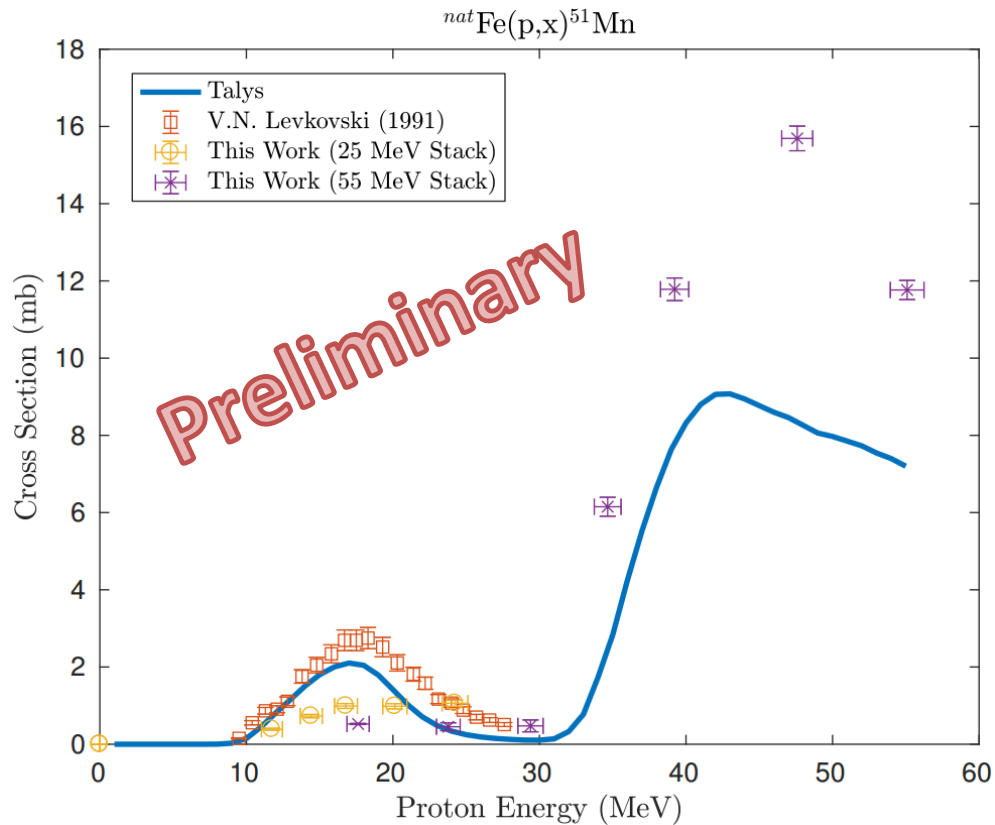
A. Springer

L. Bernstein



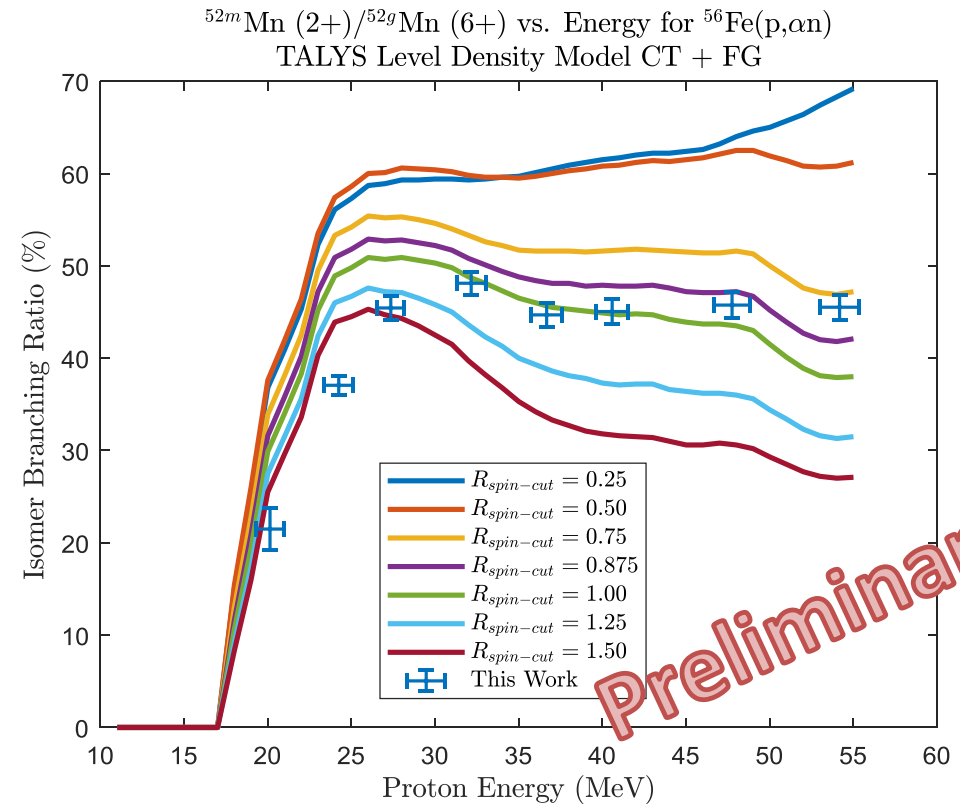
Two overlapping stacks: $E_p = 55 \rightarrow 21$ MeV,
 $25 \rightarrow 11$ MeV (120 nA@10 min, 100 nA@20 min)

$^{nat}\text{Fe}(p,x)^{51,52}\text{Mn}$ – Novel PET imaging



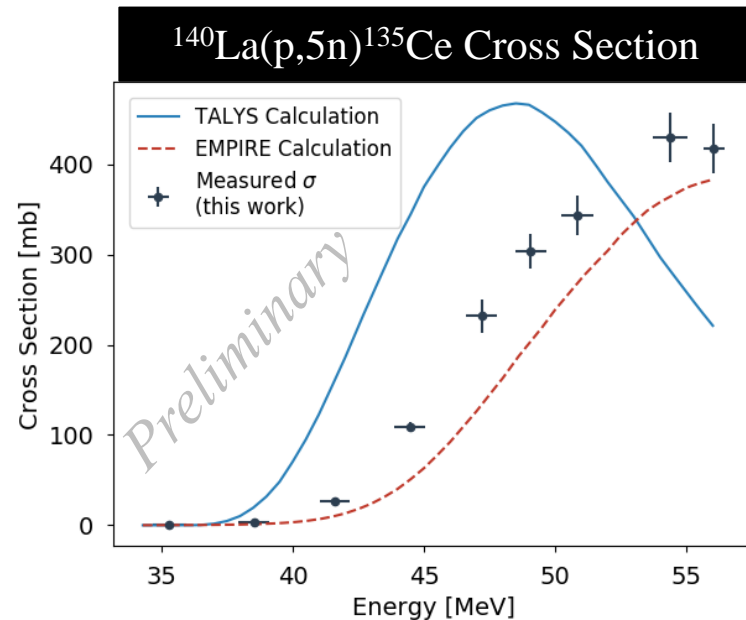
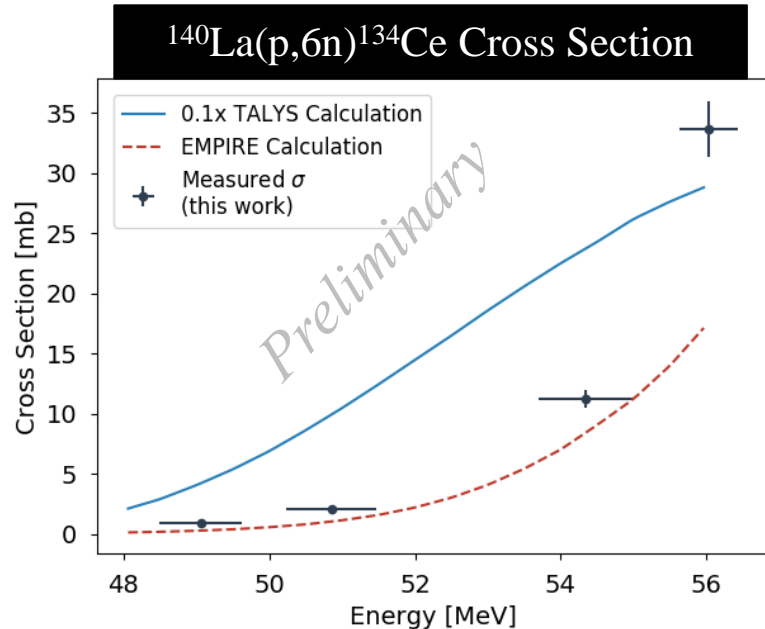
Results consistent with $R \approx 1$ at high energy. At low energy, results are ambiguous due to energy straggling.

- Emerging medical radionuclides
 - ^{51}Mn ($t_{1/2} = 46$ min, 97% β^+) – short-lived PET tracer for metabolic studies
 - ^{52g}Mn ($t_{1/2} = 5.6$ d, 29% β^+) – long-lived PET tracer for neuron tracking, immune studies



$^{140}\text{La}(p,6n)^{134}\text{Ce}$ - a PET analogue for ^{225}Ac

Go see the poster!

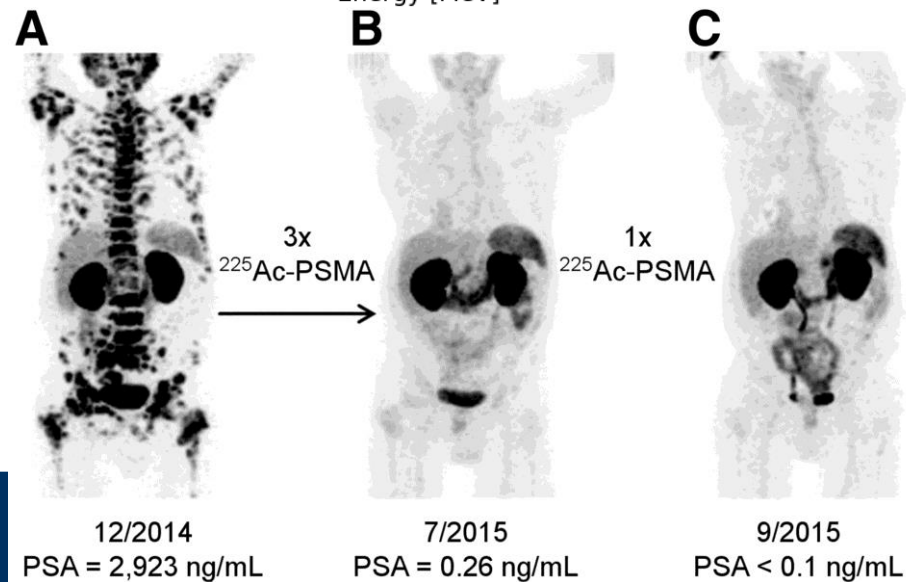


Jon Morrell

^{135}Ce is a contaminant isotope: higher-energy beam required for clean production of ^{134}Ce

Investigating potential for $^{226}\text{Ra}(n,2n)^{225}\text{Ra} \rightarrow ^{225}\text{Ac}$

Kratochwil, Clemens, et al. " ^{225}Ac -PSMA-617 for PSMA-targeted α -radiation therapy of metastatic castration-resistant prostate cancer." *Journal of Nuclear Medicine* 57.12 (2016): 1941-1944.

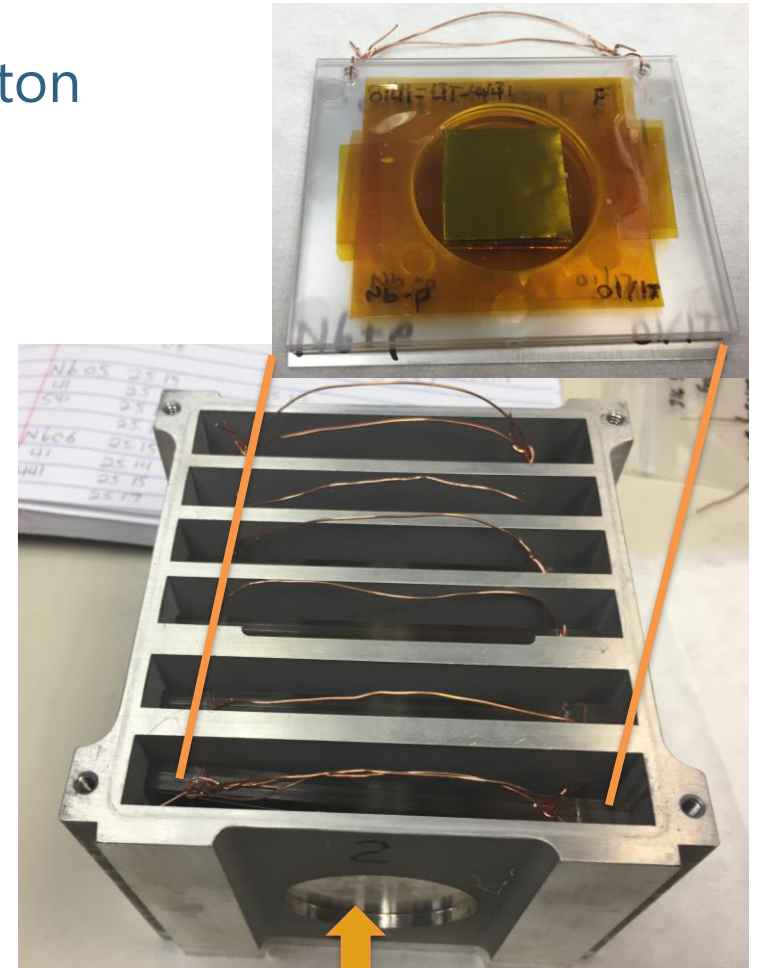
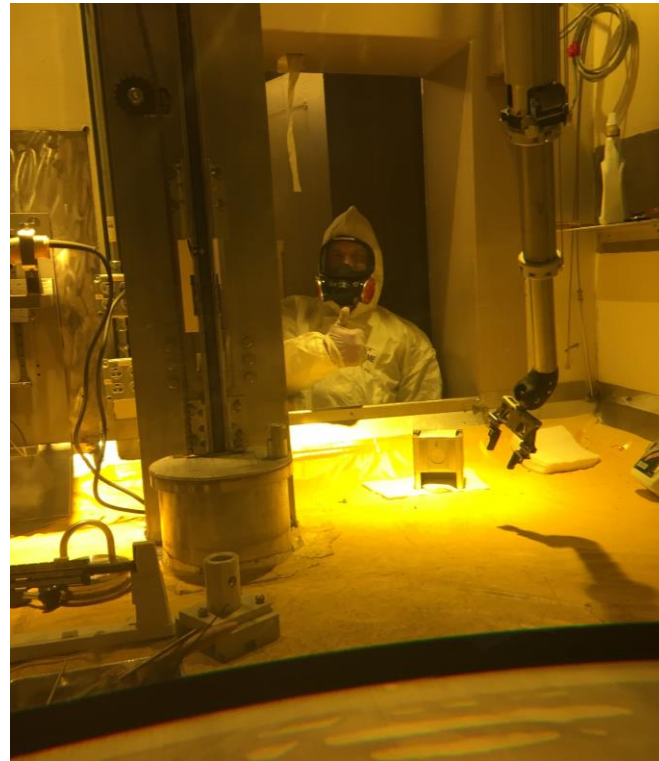
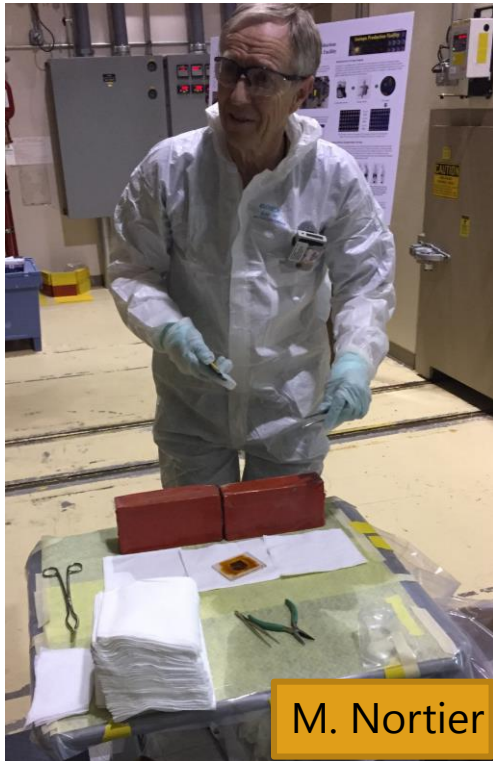


Stacked-target Charged Particle Excitation Functions

Intermediate Energy – LANL

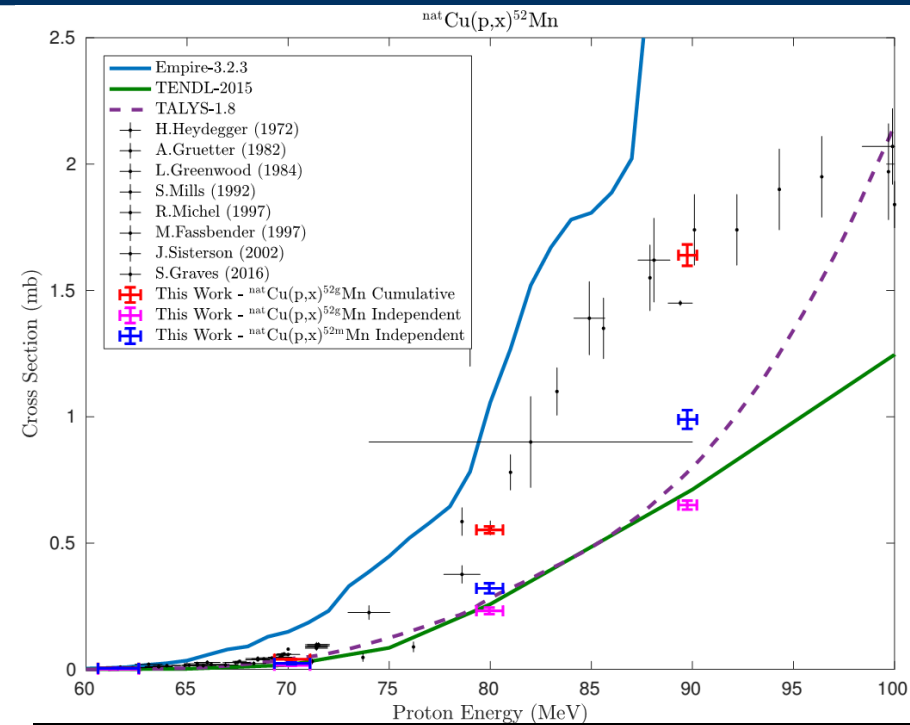
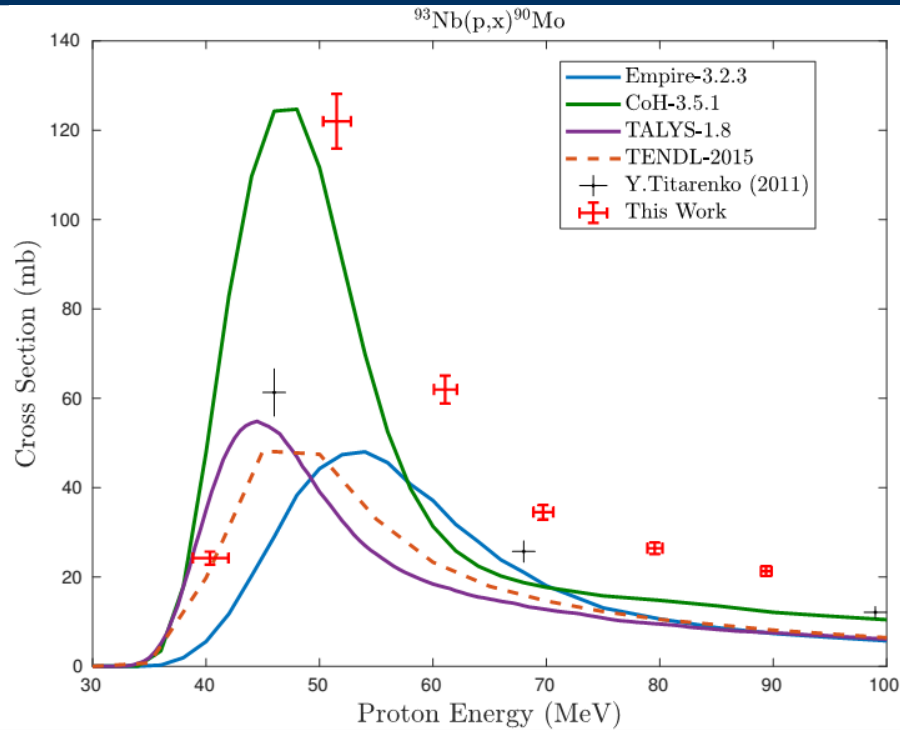
Measurements @ LANL – Nb(p,x)

- ${}^{\text{nat}}\text{Nb}(p,4n){}^{90}\text{Mo}$ is a high-priority objective as a new proton beam dosimetry standard for $E_p \approx 40 - 200$ MeV
 - Other emerging radionuclides: ${}^{82\text{m}}\text{Rb}$, ${}^{86}\text{Y}$, ${}^{89}\text{Zr}$, ${}^{90}\text{Nb}$



100 MeV p+ 100 nA @ 3 hr

Measurements @ LANL – Nb(p,x)

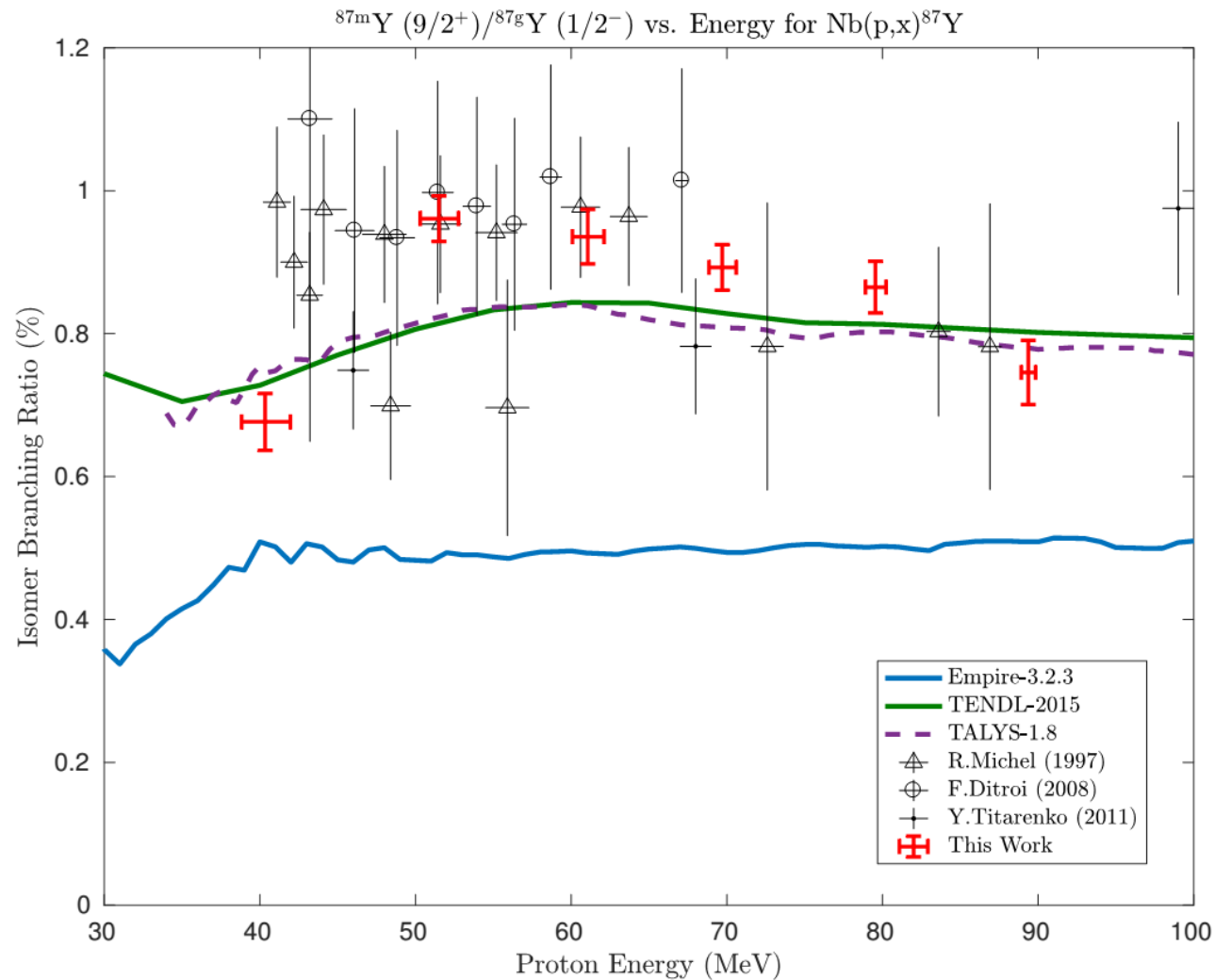


Measurements of 38 cross-sections for $^{93}\text{Nb}(p,x)$ and $^{\text{nat}}\text{Cu}(p,x)$

A.S. Voyles et al., "Excitation functions for (p,x) reactions of niobium in the energy range of $E_p = 40\text{--}90\text{ MeV}$ ", NIM B (Accepted, In Press, 2018)

$\epsilon + \beta^+$			^{90}Mo			$^{93\text{m}}\text{Mo}$	^{94}Mo	
IT			$^{89\text{m}}\text{Nb}$ ^{89}Nb	^{90}Nb	$^{91\text{m}}\text{Nb}$	$^{92\text{m}}\text{Nb}$	^{93}Nb	100 MeV p+
	^{86}Zr	^{87}Zr	^{88}Zr	^{89}Zr				
		$^{85\text{m}}\gamma$ $^{85}\gamma$	$^{86}\gamma$	$^{87\text{m}}\gamma$ $^{87}\gamma$	$^{88}\gamma$			
^{83}Sr		$^{85\text{m}}\text{Sr}$						
$^{82\text{m}}\text{Rb}$								β^-

Measurements @ LANL – Nb(p,x)



5 independent measurements of isomer-to-ground state ratios

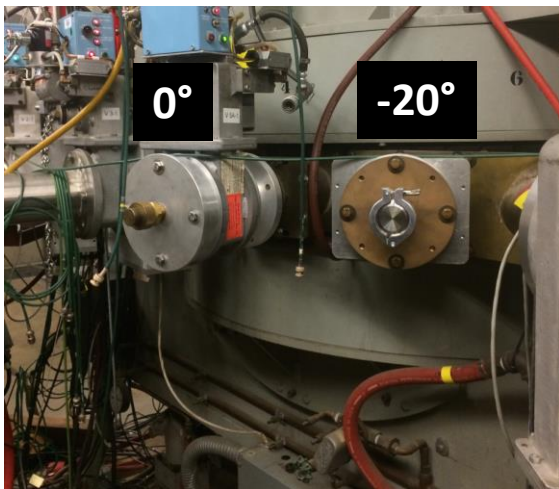


A. Lewis

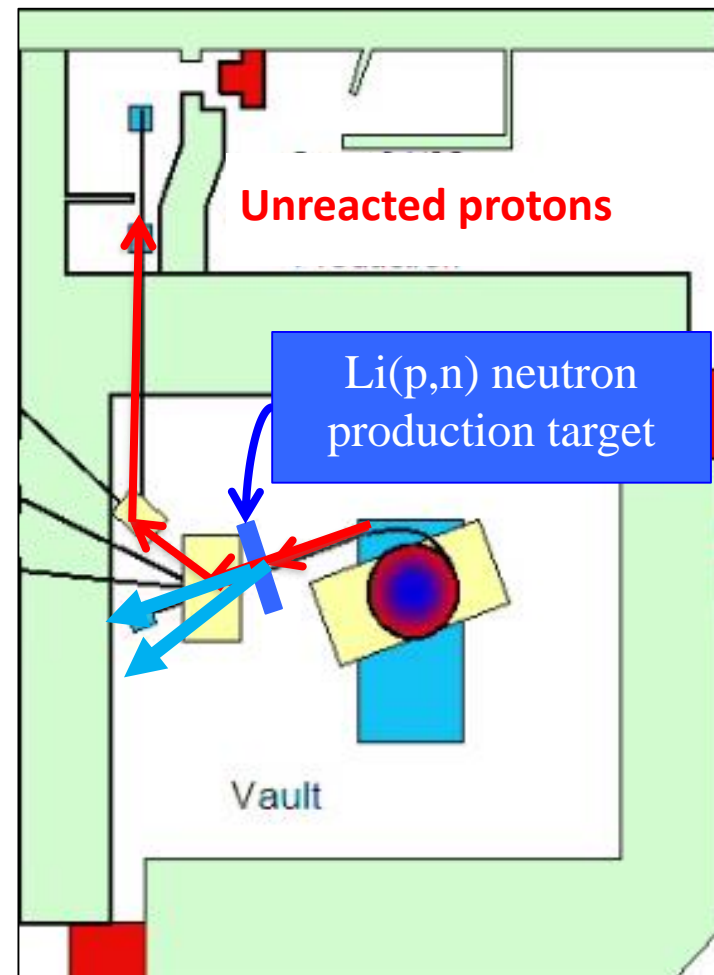
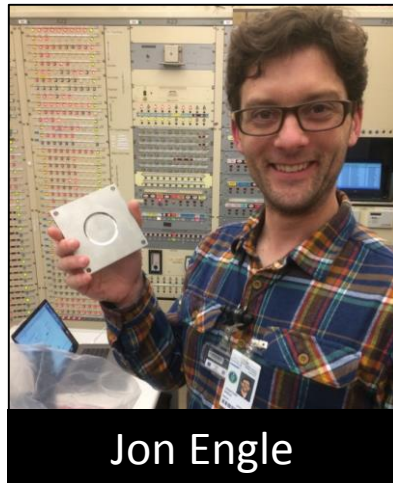
Alternative (n,x) Production Capabilities at the 88-Inch Cyclotron

${}^7\text{Li}(p,n)$ “Quasi-Monoenergetic” Neutron Source

Vault-based irradiation



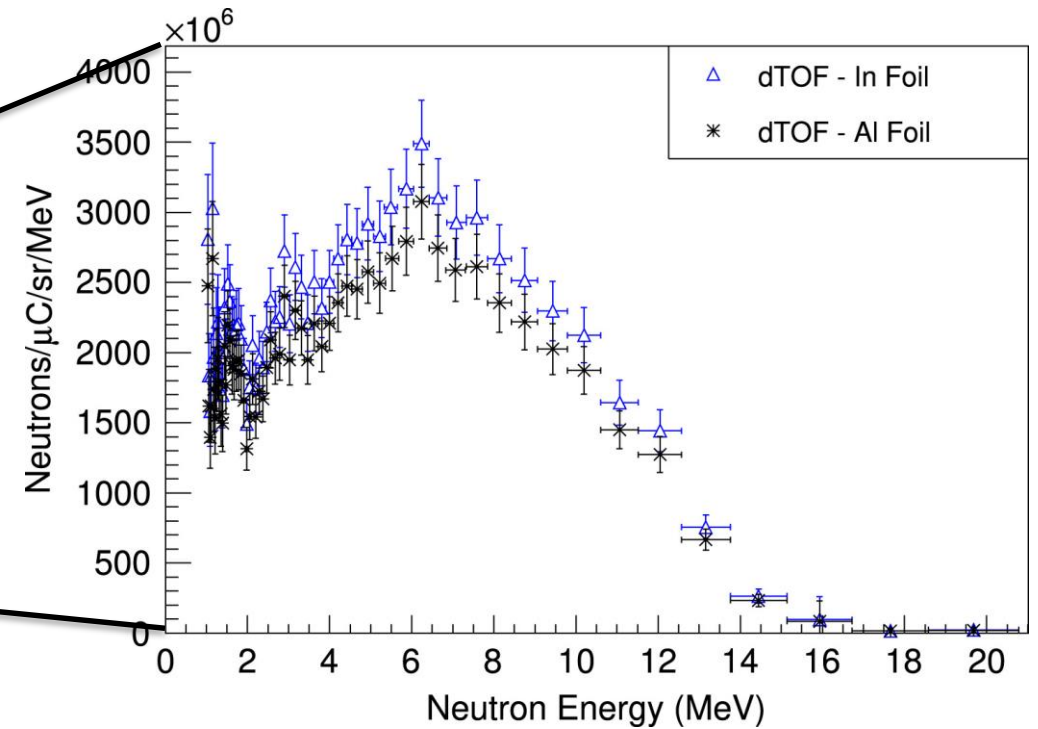
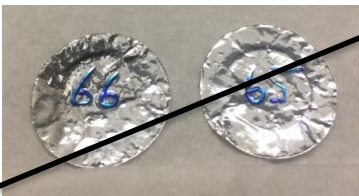
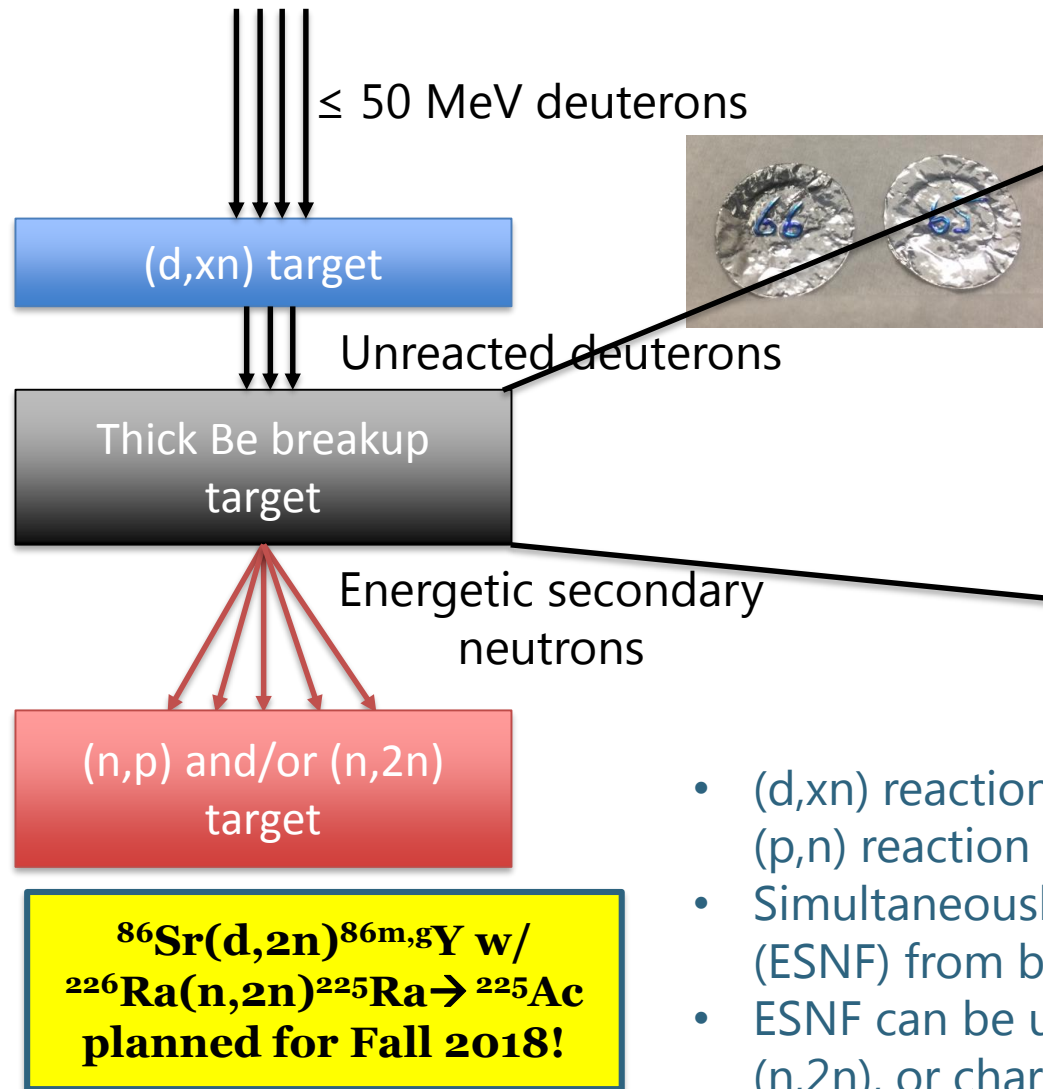
Inconel-clad Li targets
(LANL LDRD)



- Neutrons from 0-**60** MeV
- Y, Co, Al, In, Zr, Au samples irradiated in the vault
- Unreacted beam dumped in Cave 0
- Flux from 10^{6-4} /MeV/sr/s (decreases w/ E_n)

First experiments took place in April 2018

Simultaneous Radionuclide Production

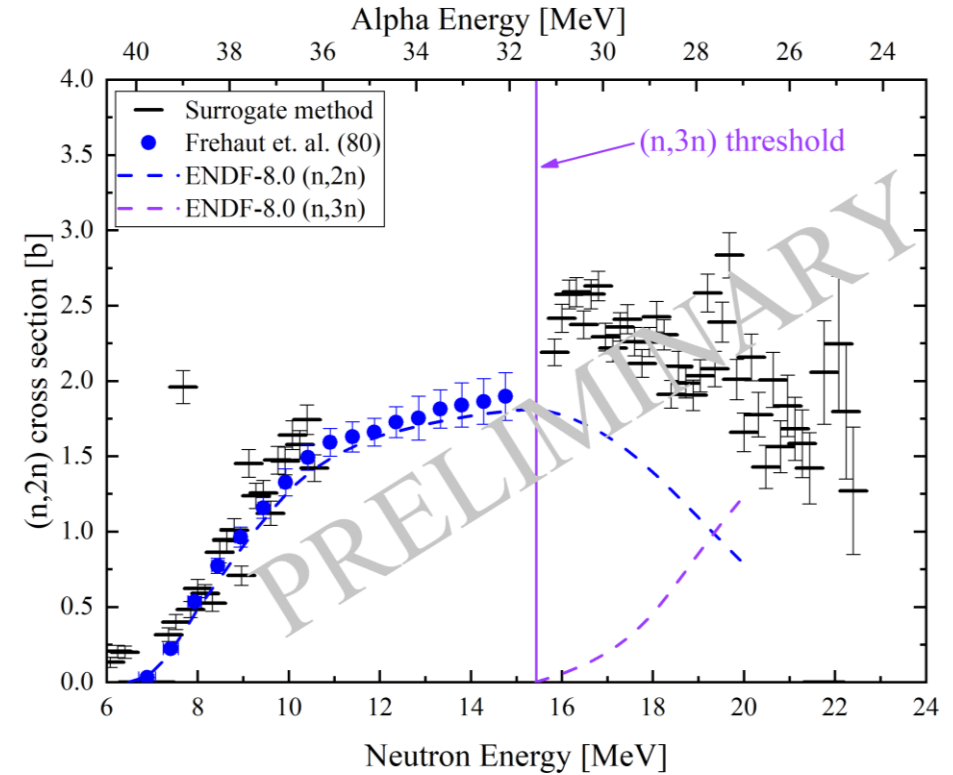
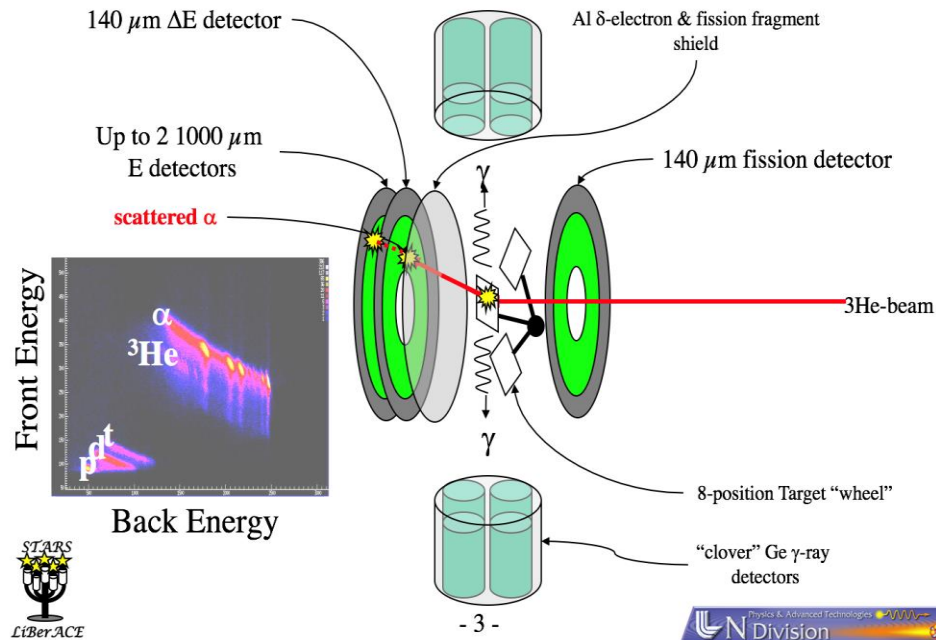


- (d,xn) reaction produces the same radionuclide as the commonly-used (p,n) reaction
- Simultaneously makes a significant energetic secondary neutron flux (ESNF) from breakup of unreacted primary deuteron beam.
- ESNF can be used to produce high specific-activity radionuclides via (n,2n), or charge exchange reactions such as (n,p) and (n,α).

$^{155}\text{Gd}(n,2n)$ Surrogate Cross-Section Measurement

$^{155}\text{Gd}(n,2n)$ cross section by measurement of surrogate reaction $^{157}\text{Gd}(^3\text{He},\alpha 2n)^{154}\text{Gd}$

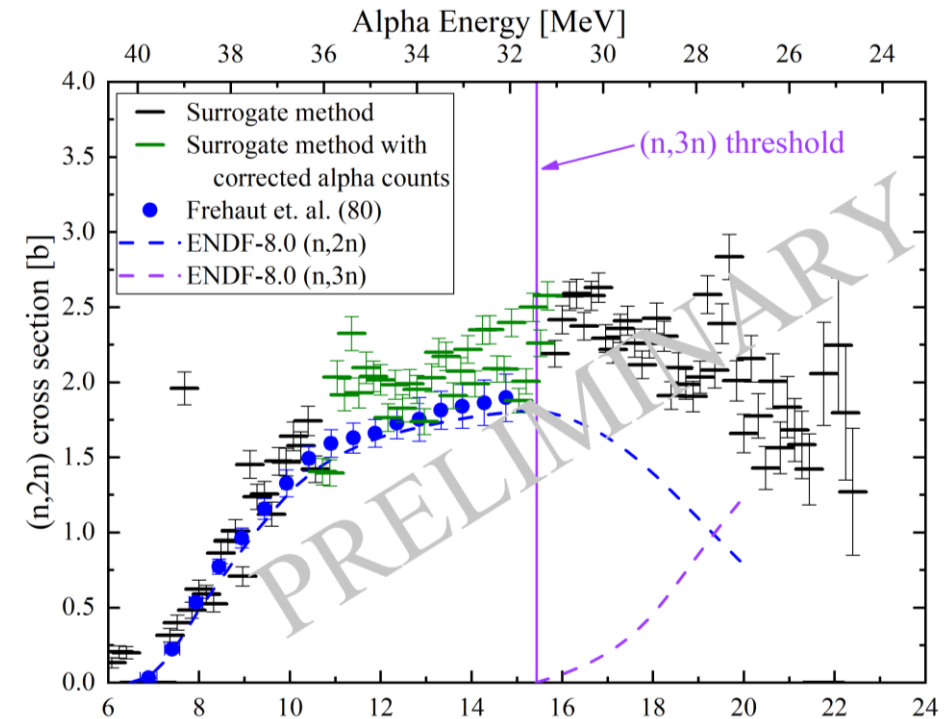
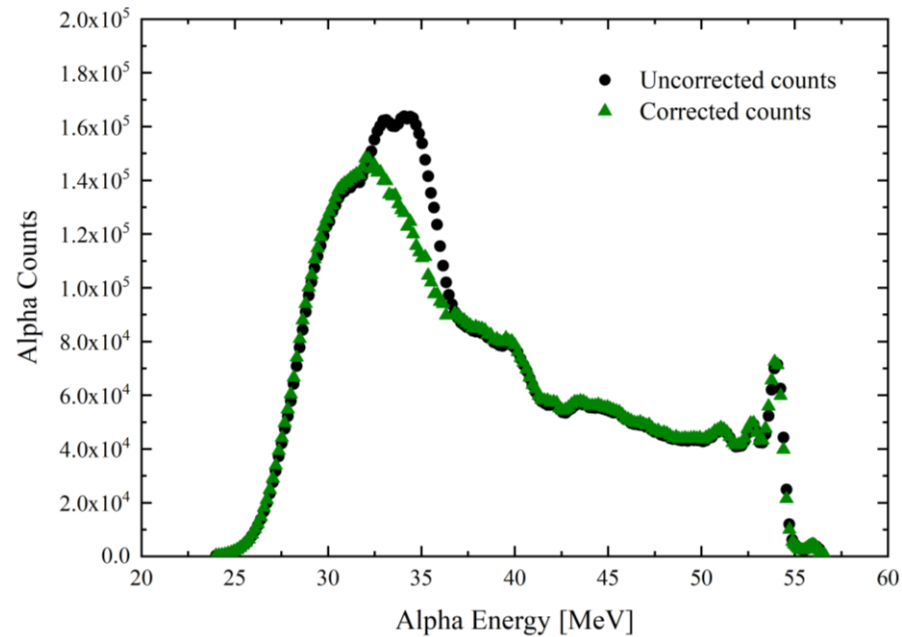
- The LiBerACE detector setup was used with $\Delta E/E$ detectors for the alphas and clover detectors for the gammas
- 123 keV and 815 keV gamma lines were used to calculate a cross section for $^{155}\text{Gd}(n,2n)$
- Work is currently being done to re-analyze the gamma data



Darren Bleuel, 10/27/06 APS/DNP Meeting presentation

$^{155}\text{Gd}(n,2n)$ cross section by measurement of surrogate reaction $^{157}\text{Gd}(^3\text{He},\alpha 2n)^{154}\text{Gd}$

- The alpha spectrum was corrected where there was contamination from carbon and oxygen reactions
- The errors presented are **statistical only** – the full error analysis has not yet been done.



E. Matthews



A. Lewis

FIER

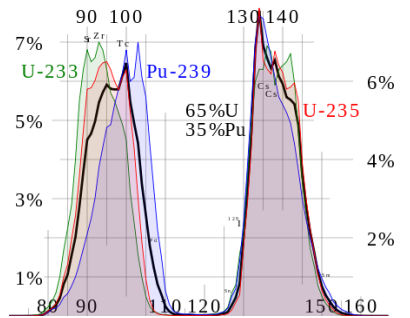
Input Data

INPUTS

Decay/Structure

ENDF B-VII.0
(ENDF File 8 / ENSDF)

Fission Yields



(England and Rider)

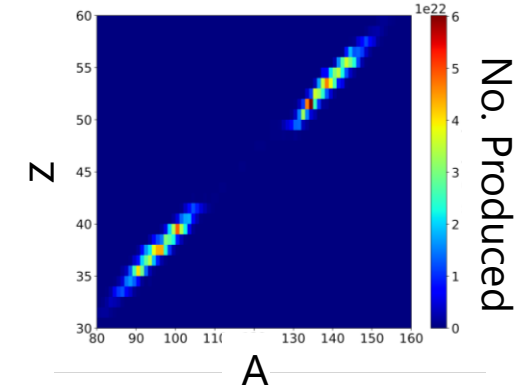


FIER

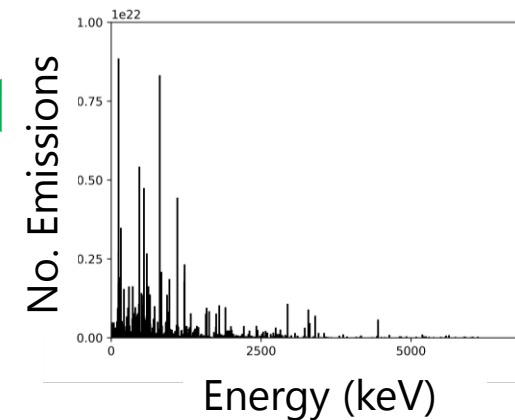
E. Matthews

Go see the poster!

Population Data



Gamma-Ray Spectra

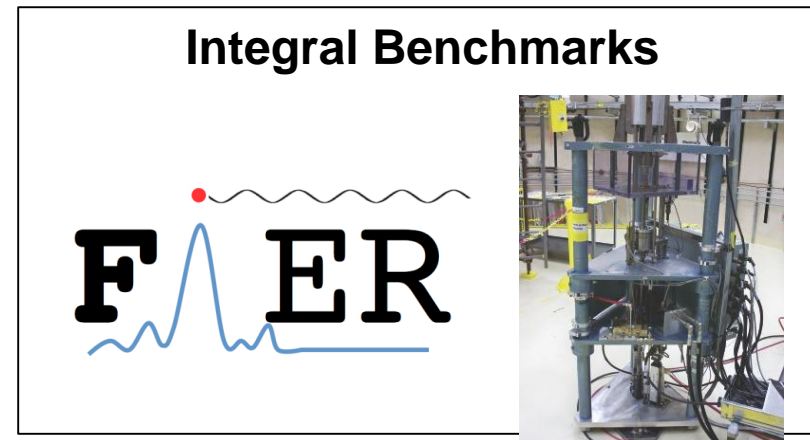
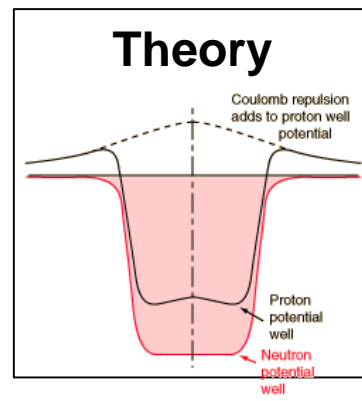
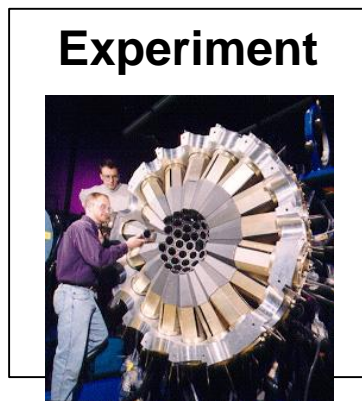


Because FIER uses an analytical and exact model for production and decay of fission products, the accuracy of FIER outputs are only dependent on nuclear data. This makes FIER ideal for sensitivity studies.

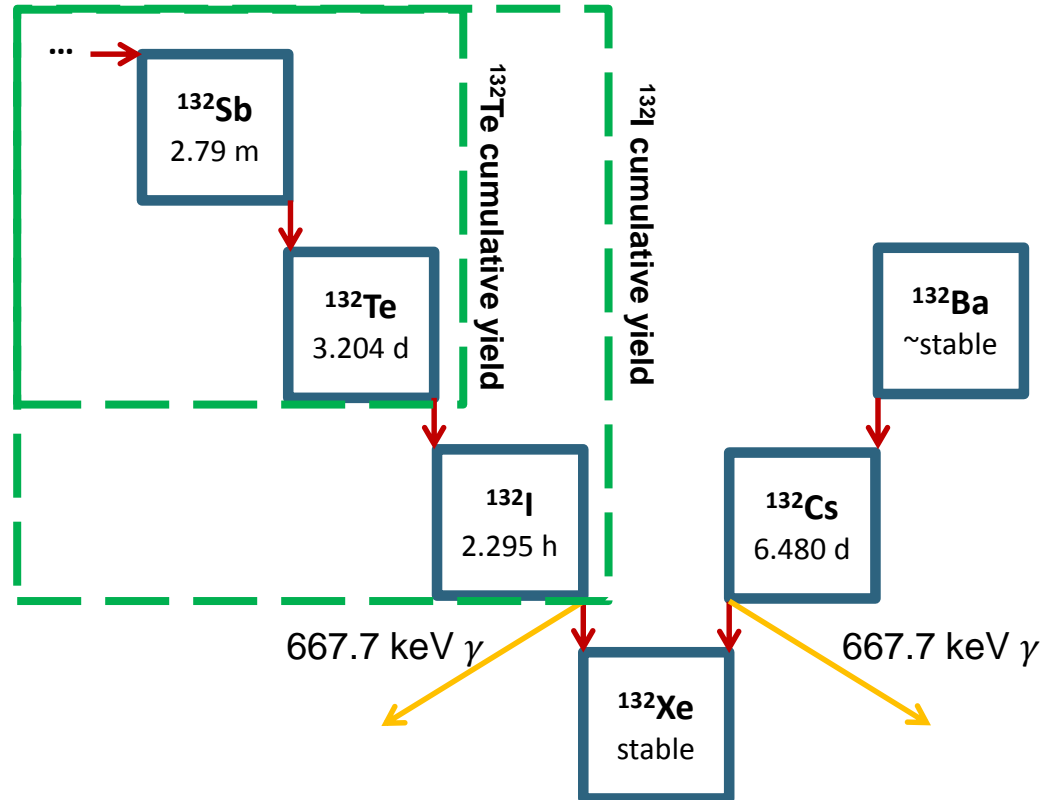
Integral Benchmarking with FIER

The experimental work presented shows how FIER is an integral calculation, making it ideal for use in integral benchmarking suites for nuclear data.

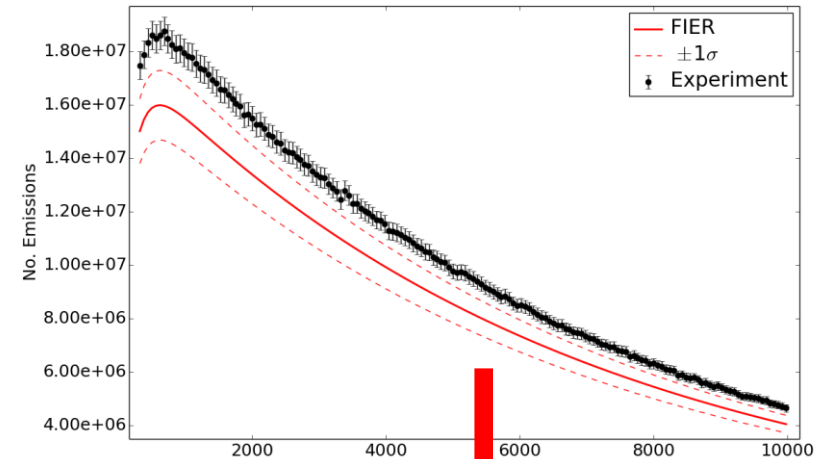
- Fission yields and decay/structure data that are input to FIER should be tuned such that they reproduce high quality delayed gamma-ray data.



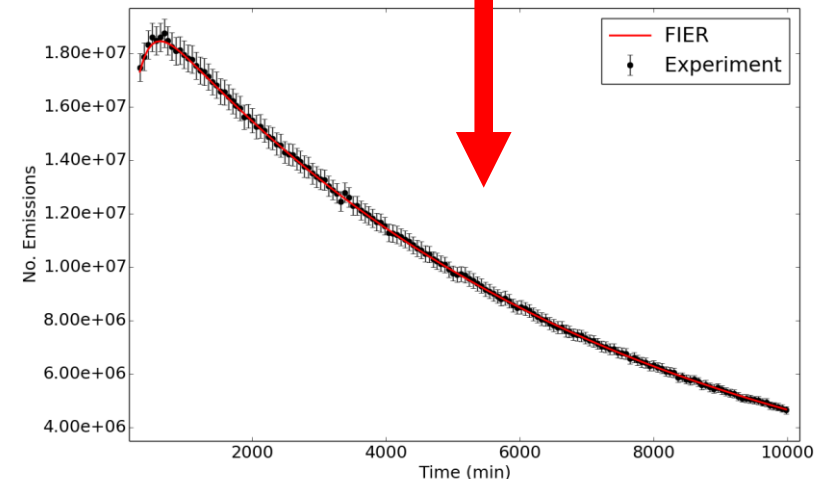
Case Study: Integral Benchmarking



- The cumulative yield of ^{132}I has a large value at 4.67% with a relative uncertainty of 64%. Thus this fission yield is possibly the source of the magnitude offset between the gamma emission predicted by FIER and the experiment.
- Demonstrates how FIER can be used to both investigate fission yield inaccuracies and provide improved values.



Increasing the fission yield of ^{132}I by 0.24σ to 5.39% resolves the discrepancy!



Collaborators on this work

M.S. Basunia¹, J.A. Batchelder², T. Bates², J.D. Bauer³, T.A. Becker⁴, L.A. Bernstein^{1,2}, E.R. Birnbaum⁵, S. Chong², J.W. Engle^{5,6}, R.B. Firestone¹, S.A. Graves⁷, A.M. Hurst¹, T. Kawano⁵, L. Kirsch³, A.M. Lewis², E.F. Matthews², F.M. Nortier⁵, P.R. Renne⁴, D. Rutte⁴, A. Springer⁸, M.A. Unzueta², K.A. Van Bibber², A.S. Voyles², C.S. Waltz³, H. Zaneb⁹

¹ Lawrence Berkeley National Laboratory

² University of California-Berkeley Dept. of Nuclear Engineering

³ Lawrence Livermore National Laboratory

⁴ Berkeley Geochronology Center

⁵ Los Alamos National Laboratory

⁶ University of Wisconsin – Madison

⁷ University of Iowa – Department of Radiation Oncology

⁸ Karlsruhe Institute of Technology

⁹ University of Lahore



Tusen takk!